

Prediction of e^\pm elastic scattering cross-section ratio based on phenomenological two-photon exchange corrections

I. A. Qattan

Khalifa University of Science and Technology, Department of Physics, P.O. Box 127788, Abu Dhabi, United Arab Emirates

(Received 5 March 2017; revised manuscript received 24 April 2017; published 14 June 2017)

I present a prediction of the e^\pm elastic scattering cross-section ratio, $R_{e^+e^-}$, as determined using a new parametrization of the two-photon exchange (TPE) corrections to electron-proton elastic scattering cross section σ_R . The extracted ratio is compared to several previous phenomenological extractions, TPE hadronic calculations, and direct measurements from the comparison of electron and positron scattering. The TPE corrections and the ratio $R_{e^+e^-}$ show a clear change of sign at low Q^2 , which is necessary to explain the high- Q^2 form factors discrepancy while being consistent with the known $Q^2 \rightarrow 0$ limit. While my predictions are in generally good agreement with previous extractions, TPE hadronic calculations, and existing world data including the recent two measurements from the CLAS and VEPP-3 Novosibirsk experiments, they are larger than the new OLYMPUS measurements at larger Q^2 values.

DOI: [10.1103/PhysRevC.95.065208](https://doi.org/10.1103/PhysRevC.95.065208)

I. INTRODUCTION

The electromagnetic form factors of the proton and neutron, $G_E^{(p,n)}$ and $G_M^{(p,n)}$, are fundamental quantities which provide information on the spatial distributions of charge and magnetization within nucleons. The form factors are measured using electron scattering where the incident electron scatters from a nucleon target through the exchange of a virtual photon. By increasing the four-momentum transferred squared of the virtual photon, Q^2 , the virtual photon becomes more sensitive to the small scale internal structure of the nucleon.

Primarily, there are two methods used to extract the proton form factors. The first is the Rosenbluth or longitudinal-transverse (LT) separation method [1], which relies on measurements of the unpolarized cross section. The second is the polarization transfer or polarized target (PT) method [2], which requires measurement of the spin-dependent cross section.

In the Rosenbluth separation method, the reduced cross section σ_R for electron-proton elastic scattering in the Born or one-photon exchange (OPE) approximation is given by

$$\sigma_R = (G_M^p(Q^2))^2 + \frac{\varepsilon}{\tau} (G_E^p(Q^2))^2, \quad (1)$$

where $\tau = Q^2/4M_p^2$ is a kinematics factor, M_p is the mass of the proton, and ε is the virtual photon longitudinal polarization parameter, defined as $\varepsilon^{-1} = [1 + 2(1 + \tau) \tan^2(\frac{\theta_e}{2})]$, where θ_e is the scattering angle of the electron. For a fixed Q^2 value, measuring σ_R at several ε points, one can separate G_E^p and G_M^p . For cases where ε/τ is small (large), extraction of G_E^p (G_M^p) with high precision would be difficult.

In the recoil polarization method, a beam of longitudinally polarized electrons scatters elastically from the unpolarized proton target. The electrons transfer their polarization to the unpolarized protons. Simultaneous measurements of the transverse, P_t , and longitudinal, P_l , polarization components of the recoil proton, allows for the determination of the ratio

$\mu_p G_E^p/G_M^p$ in the OPE [2–4]:

$$\mu_p R = \mu_p \frac{G_E^p}{G_M^p} = -\frac{P_t (E + E')}{P_l 2M_p} \tan\left(\frac{\theta_e}{2}\right), \quad (2)$$

where E and E' are the initial and final energy of the incident electron, respectively. The ratio can be extracted in a similar fashion using polarized beams and targets by measuring the asymmetry for two different spin directions [5,6].

A significant difference is observed between LT and PT extractions of the proton form factors [5–22]. The values of $\mu_p G_E^p/G_M^p$ differ almost by a factor of three at high Q^2 . In the LT separation method, the ratio shows approximate form factor scaling, $\mu_p G_E^p/G_M^p \approx 1$, albeit with large uncertainties at high Q^2 values. The recoil polarization method yields a ratio that decreases roughly linearly with increasing Q^2 , with some hint of flattening out above 5 (GeV/c)².

Several studies suggested that missing higher order radiative corrections to σ_R , and in particular, larger-than-expected TPE contributions [23–27] diagrams may explain the discrepancy. The impact of TPE effects was studied both theoretically [28–33] and phenomenologically [25,34–45]. Most studies suggested that the TPE corrections are relatively small, but have a significant angular dependence which mimics the effect of a larger value of G_E^p . See Refs. [23,24] for detailed reviews.

To account for TPE contributions to σ_R , I add the real function $F(\varepsilon, Q^2)$ to the Born reduced cross section

$$\sigma_R = (G_M^p)^2 \left[1 + \frac{\varepsilon}{\tau} R^2 \right] + F(\varepsilon, Q^2), \quad (3)$$

where $R = G_E^p/G_M^p$ is the recoil polarization ratio.

Experimentally, several measurements were performed to verify the discrepancy [7,8]. The goal was to measure or constrain TPE contributions to σ_R and hence the ratio $\mu_p G_E^p/G_M^p$. Several studies examined the ε dependence of σ_R [35–37], and no deviation from linearity as predicted in the OPE approximation was observed. Meziane and collaborators [46] performed a measurement to look for TPE effects by extracting the ratio $\mu_p G_E^p/G_M^p$ at $Q^2 = 2.50$ (GeV/c)² as a function

of scattering angle. However, no deviation from the OPE prediction was observed as the result should be independent of scattering angle in the Born approximation.

Several analyses were performed to extract the TPE contributions based on the observed discrepancy between the LT and PT results. With the assumption that TPE contributions are linear in ε and vanish in the forward limit ($\varepsilon \rightarrow 1$) (Regge limit) [37,47], and that the PT results were confirmed experimentally to be independent of ε , extractions of the TPE contribution using combined cross section and polarization measurements of elastic electron-proton scattering were also performed [25,37–39,41–44,48]. Several analyses also attempted to extract the TPE amplitudes with fewer assumptions [40,49,50], though with relatively large uncertainties.

The most direct technique for measuring TPE is the comparison of electron-proton and positron-proton scattering. The function $F(\varepsilon, Q^2)$ which represents the interference of the OPE and TPE amplitudes, changes sign depending on the charge of the projectile (lepton), yielding an amplified signal when taking the ratio of electron and positron scattering. Therefore, any deviation of the ratio $R_{e^+e^-}(Q^2, \varepsilon)$ defined as

$$R_{e^+e^-}^{\text{raw}}(\varepsilon, Q^2) = \frac{\sigma(e^+p \rightarrow e^+p)}{\sigma(e^-p \rightarrow e^-p)}, \quad (4)$$

from unity will be a direct evidence for the TPE effect and therefore provides a direct way to determine its magnitude. The ratio $R_{e^+e^-}$ can be expressed as $R_{e^+e^-} \approx 1 + 4\Re(A_{2\gamma})/A_{1\gamma}$ with $A_{1\gamma}$ and $A_{2\gamma}$ being the OPE and TPE amplitudes [51], respectively. Here \Re stands for the real part. On the other hand, the modification to the electron cross section is $\approx 1 - 2\Re(A_{2\gamma})/A_{1\gamma}$. Clearly, any change in the electron cross section will have almost twice the change in the ratio $R_{e^+e^-}$ but with opposite sign.

The only other first-order radiative correction which depends on the lepton sign is the interference between diagrams with Bremsstrahlung from the electron and proton, and this contribution is generally small. Therefore, after correcting for the electron-proton Bremsstrahlung interference term and the conventional charge-independent radiative corrections, the ratio $R_{e^+e^-}$ becomes

$$R_{e^+e^-}(\varepsilon, Q^2) = \frac{1 - \delta_{2\gamma}}{1 + \delta_{2\gamma}} \approx 1 - 2\delta_{2\gamma}, \quad (5)$$

where $\delta_{2\gamma} = F(\varepsilon, Q^2)/\sigma_{\text{Born}}$ is the fractional TPE correction for electron-proton scattering, and σ_{Born} is the Born reduced cross section.

Until recently, there was only limited evidence for any nonzero TPE contribution from such comparisons [52], as data were limited to low Q^2 or large ε , where the TPE contributions appear to be small. In addition, the details of the radiative corrections applied to these earlier measurements are not always available, and it is not clear if the charge-even corrections were applied in all cases. New measurements by the CLAS collaboration [53] and the VEPP-3 collaboration [54] have found more significant indications of TPE contributions at low ε and moderate Q^2 , with the ratio $R_{e^+e^-}$ larger than unity. This is consistent with a variety of TPE calculations which include the effect of hadronic structure [29,33,55,56] in somewhat

different approximations, but has the opposite sign compared to the exact calculations at $Q^2 = 0$ (or the high proton mass limit) [57], and finite- Q^2 calculations for a point-proton [24]. It is important to mention here that the VEPP-3 data are normalized to the luminosity normalization points taken at small scattering angles (high ε) which assumed $R_{e^+e^-} = 1$. This clearly was not a good assumption as demonstrated later by the new OLYMPUS data [58]. Therefore, the VEPP-3 data should be shifted such as the normalization point used is at the $R_{e^+e^-}$ value of the prediction curve to which the data are compared. Recently, new precision measurements of the ratio $R_{e^+e^-}$ by the OLYMPUS collaboration [58] at Q^2 values of 0.165–2.038 (GeV/c)² showed that $R_{e^+e^-}$ is less than unity at high ε and gradually increased to about 2% at $\varepsilon = 0.46$. Their results were generally below TPE calculations of Blunden [59], but in reasonable agreement with subtracted dispersion calculation of Tomalak [60] and Bernauer's phenomenological fit [48]. These three recent experiments measured the ratio $R_{e^+e^-}$ for $Q^2 < 2.1$ (GeV/c)², and their results are in good agreement with each other within statistical and systematic uncertainties. However, the VEPP-3 results show a sharper Q^2 dependence which disappears mostly when the results are compared to calculations that increase with Q^2 . See Ref. [61] for latest review of TPE contributions to elastic electron-proton scattering.

II. TWO-PHOTON EXCHANGE CONTRIBUTION

Based on the formalism of Guichon and Vanderhaeghen [25], Guttman and collaborators [40] expressed the reduced cross section $\sigma_R/G_{M_p}^2$, the ratio $-\mu_p\sqrt{\tau(1+\varepsilon)}/(2\varepsilon)P_t/P_l$, and the ratio P_l/P_l^{Born} in terms of the ratio G_E^p/G_M^p and the real parts of the TPE amplitudes relative to the magnetic form factor or $Y_M(\varepsilon, Q^2) = \Re(\delta\tilde{G}_M^p/G_M^p)$, $Y_E(\varepsilon, Q^2) = \Re(\delta\tilde{G}_E^p/G_M^p)$, and $Y_3(\varepsilon, Q^2) = (\nu/M_p^2)\Re(\tilde{F}_3/G_M^p)$ as

$$\frac{\sigma_R}{(G_M^p)^2} = 1 + \frac{\varepsilon}{\tau} \left(\frac{G_E^p}{G_M^p} \right)^2 + 2Y_M + \frac{2\varepsilon}{\tau} \frac{G_E^p}{G_M^p} Y_E + 2\varepsilon \left(1 + \frac{G_E^p}{\tau G_M^p} \right) Y_3 + O(e^4), \quad (6a)$$

$$-\sqrt{\frac{\tau(1+\varepsilon)}{2\varepsilon}} \frac{P_t}{P_l} = \frac{G_E^p}{G_M^p} + Y_E - \frac{G_E^p}{G_M^p} Y_M + \left(1 - \frac{2\varepsilon}{1+\varepsilon} \frac{G_E^p}{G_M^p} \right) Y_3 + O(e^4), \quad (6b)$$

$$\frac{P_l}{P_l^{\text{Born}}} = 1 - 2\varepsilon \left(1 + \frac{\varepsilon}{\tau} \left(\frac{G_E^p}{G_M^p} \right)^2 \right)^{-1} \times \left\{ \left[\frac{\varepsilon}{1+\varepsilon} \left(1 - \frac{1}{\tau} \left(\frac{G_E^p}{G_M^p} \right)^2 \right) + \frac{G_E^p}{\tau G_M^p} \right] Y_3 + \frac{G_E^p}{\tau G_M^p} \left[Y_E - \frac{G_E^p}{G_M^p} Y_M \right] \right\} + O(e^4). \quad (6c)$$

TABLE I. Values of the fit parameters for the TPE amplitudes coefficients $\alpha_{(0,1,2)}(Q^2)$ and $\beta_{(0,1,2)}(Q^2)$. The reduced χ^2 value of the fit is also listed.

Coefficient	α_0	α_1	α_2	χ_v^2
$\alpha_0(Q^2)$	$(-0.89 \pm 1.27) \times 10^{-3}$	$(-1.45 \pm 0.80) \times 10^{-2}$	$(+7.75 \pm 2.59) \times 10^{-3}$	1.56
$\alpha_1(Q^2)$	$(-0.58 \pm 0.86) \times 10^{-3}$	$(+1.02 \pm 0.53) \times 10^{-2}$	$(-3.77 \pm 0.17) \times 10^{-3}$	1.36
$\alpha_2(Q^2)$	$(+1.22 \pm 0.80) \times 10^{-3}$	$(+3.95 \pm 5.47) \times 10^{-3}$	$(-3.78 \pm 1.87) \times 10^{-3}$	1.92
$\beta_0(Q^2)$	$(+3.19 \pm 1.43) \times 10^{-3}$	$(+5.53 \pm 8.30) \times 10^{-3}$	$(-5.88 \pm 2.69) \times 10^{-3}$	1.57
$\beta_1(Q^2)$	$(-2.56 \pm 0.85) \times 10^{-3}$	$(-0.02 \pm 4.98) \times 10^{-3}$	$(+1.51 \pm 1.58) \times 10^{-3}$	1.28
$\beta_2(Q^2)$	$(-1.49 \pm 0.89) \times 10^{-3}$	$(-3.93 \pm 5.85) \times 10^{-3}$	$(+3.94 \pm 2.00) \times 10^{-3}$	1.91

Recently [50] I have extracted the three TPE amplitudes Y_M , Y_E , and Y_3 (generalized form factors) as a function of ε at fixed Q^2 value using Eqs. (6a)–(6c) above. Summary of the procedure, together with the constraints and assumptions used is outlined below:

(1) I assumed that the TPE correction is responsible mainly for the discrepancy between the cross section and polarization data measurements.

(2) The recoil polarization data were confirmed “*experimentally*” to be independent of ε [46]. Therefore, I constrain the ratio $-\sqrt{\tau}(1+\varepsilon)/(2\varepsilon)P_l/P_l$ in Eq. (6b) to its ε -independent term (Born value) or $R = G_E^p/G_M^p$ by setting the TPE contributions to zero. In this case the amplitude $Y_M(\varepsilon, Q^2)$ can be expressed in terms of the remaining $Y_E(\varepsilon, Q^2)$ and $Y_3(\varepsilon, Q^2)$ amplitudes. In addition, I used the recent improved parametrization of the ratio $R = G_E^p/G_M^p$ along with its associated uncertainty [44] from polarization measurements at both low- and high- Q^2 values

$$\mu_p R = \frac{1}{1 + 0.1430Q^2 - 0.0086Q^4 + 0.0072Q^6} \quad (7)$$

with an absolute uncertainty in the fit given by $\delta_R^2(Q^2) = \mu_p^{-2}[(0.006)^2 + (0.015\ln(1+Q^2))^2]$, with Q^2 in $(\text{GeV}/c)^2$. Therefore, $\sigma_R/(G_M^p)^2$ as given by Eq. (6a) is written as

$$\begin{aligned} \frac{\sigma_R}{(G_M^p)^2} = & 1 + \frac{\varepsilon}{\tau}R^2 + \left[\frac{2}{R} + \frac{2\varepsilon R}{\tau} \right] Y_E(\varepsilon, Q^2) \\ & + \left[\frac{2}{R} \left(1 - \frac{2\varepsilon R}{1+\varepsilon} \right) + 2\varepsilon \left(1 + \frac{R}{\tau} \right) \right] Y_3(\varepsilon, Q^2). \end{aligned} \quad (8)$$

(3) Because of the experimentally observed linearity of the Rosenbluth plots [34–37] where σ_R exhibits no (or weak) nonlinearity in ε , I expanded each of the amplitudes Y_E and Y_3 as a second-order polynomial to reserve as possible the linearity of σ_R as well as to account for any possible nonlinearities in the TPE amplitudes

$$\begin{aligned} Y_E(\varepsilon, Q^2) &= (\alpha_0 + \alpha_1\varepsilon + \alpha_2\varepsilon^2), \\ \text{and} \\ Y_3(\varepsilon, Q^2) &= (\beta_0 + \beta_1\varepsilon + \beta_2\varepsilon^2) \end{aligned} \quad (9)$$

with α_i and β_i ($i = 0, 1, 2$) are functions of Q^2 only.

(4) Substituting Eqs. (9) in Eq. (8), and imposing the Regge limit where the TPE correction to σ_R vanishes in the limit $\varepsilon \rightarrow 1$, one obtains $Y_E(1, Q^2) = -Y_3(1, Q^2)$ or simply $(\alpha_0 + \alpha_1 +$

$\alpha_2) = -(\beta_0 + \beta_1 + \beta_2)$. Further, to ensure the correct behavior of the TPE amplitudes as $\varepsilon \rightarrow 1$ where each amplitude must go to zero (Regge limit), one obtains the following constraints on the coefficients: $\alpha_0 = -(\alpha_1 + \alpha_2)$ and $\beta_0 = -(\beta_1 + \beta_2)$.

(5) Using the constraints on α_0 and β_0 derived above, σ_R can now be expressed as

$$\begin{aligned} \frac{\sigma_R}{(G_M^p)^2} = & 1 + \frac{\varepsilon}{\tau}R^2 + \left[\frac{2}{R} + \frac{2\varepsilon R}{\tau} \right] [\alpha_1(\varepsilon - 1) + \alpha_2(\varepsilon^2 - 1)] \\ & + \left[\frac{2}{R} \left(1 - \frac{2\varepsilon R}{1+\varepsilon} \right) + 2\varepsilon \left(1 + \frac{R}{\tau} \right) \right] \\ & \times [\beta_1(\varepsilon - 1) + \beta_2(\varepsilon^2 - 1)]. \end{aligned} \quad (10)$$

where $(G_M^p)^2$, α_1 , α_2 , β_1 , and β_2 can in principle be determined by fitting σ_R to ε for a fixed Q^2 value.

(6) In order to utilize Eq. (10) above, and for a fixed Q^2 value, σ_R must be measured at a minimum of six ε points. However, the number of fitting parameters can be reduced by fixing the value of $(G_M^p)^2$ and making use of the assumption that for $\varepsilon \rightarrow 1$, the TPE correction to σ_R vanishes or $\sigma_R(\varepsilon = 1, Q^2) = [(G_M^p)^2 + (G_E^p)^2/\tau]$. In addition, because of the experimentally observed linearity of the Rosenbluth plots where σ_R data show a linear behavior in ε suggesting the fit: $\sigma_R = [a(Q^2) + \varepsilon b(Q^2)]$. Therefore, for a fixed Q^2 value, I linearly fit σ_R to ε and extract the constants $a(Q^2)$ and $b(Q^2)$. Equating the two expressions for $\sigma_R(\varepsilon = 1, Q^2)$ yields

$$(G_M^p(Q^2))^2 = \frac{a(Q^2) + b(Q^2)}{(1 + \frac{R^2}{\tau})}. \quad (11)$$

(7) I fit the world data on σ_R used in the analysis of Ref. [44] to extract $(G_M^p(Q^2))^2$ first following Eq. (11). By constraining the values of $(G_M^p(Q^2))^2$ and the ratio R as given by Eqs. (7) and (11), respectively, I fit σ_R to Eq. (10), and extract the TPE amplitudes coefficients α_i and β_i ($i = 1, 2$), which are then used to determine the coefficients α_0 and β_0 . In the analysis, 93 Q^2 points up to $Q^2 = 4.0(\text{GeV}/c)^2$ were used with σ_R measured at a minimum of five ε points. For the high Q^2 points, $Q^2 > 1(\text{GeV}/c)^2$, the majority of σ_R measurements were made at a limited number of ε points (below five points), and therefore, only a handful of sets of these Q^2 points could be used in the analysis. However, this was not the case for the low- Q^2 measurements.

(8) The TPE amplitudes coefficients α_k and β_k ($k = 0, 1, 2$) are at the few-percentage-points level, and they were all

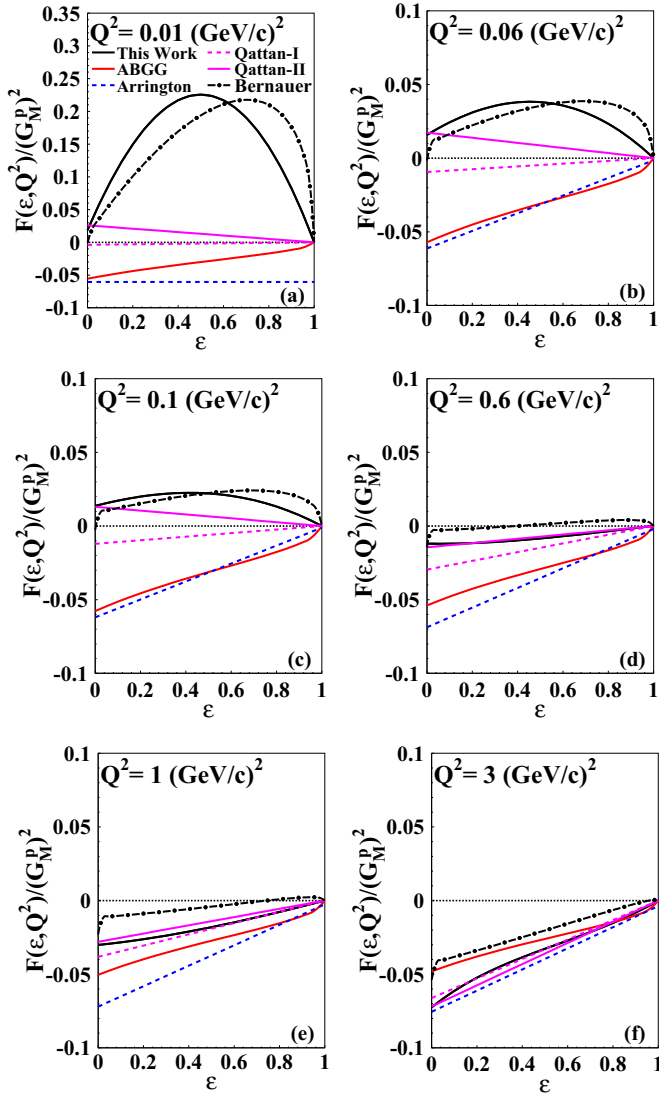


FIG. 1. The ratio $F(\epsilon, Q^2)/(G_M^p)^2$ as a function of ϵ as extracted from this work (solid black line) for a range of Q^2 values listed in the figure. Also shown are previous phenomenological extractions and fits: ABGG [62] (solid red line), Arrington [39] (dashed blue line), Qattan-I [42] (dashed magenta line), Qattan-II [44] (solid magenta line), and Bernauer [48] (dashed-dotted black line).

best parametrized as a second-order polynomial of the form: $\alpha(\beta)_{(0,1,2)}(Q^2) = (a_0 + a_1 Q^2 + a_2 Q^4)$. The parameters of the fits along with the reduced χ^2 values obtained are listed in Table I. See Ref. [50] for details.

III. RESULTS AND DISCUSSION

I use my new parametrization of the TPE amplitudes to construct the TPE contributions to electron-proton elastic scattering $F(\epsilon, Q^2)$ based on the formalism of Guichon and Vanderhaeghen [25]. Figure 1 shows the ϵ dependence of the ratio $F(\epsilon, Q^2)/(G_M^p)^2$ as extracted from this work (solid black line). In addition, I compare the results to several previous

phenomenological extractions and fits: “ABGG” [62] (solid red line), “Arrington” [39] (dashed blue line), “Qattan-I” [42] (dashed magenta line), “Qattan-II” [44] (solid magenta line), and “Bernauer” [48] (dashed-dotted black line). The ratio as extracted from this work is positive and exhibits strong nonlinearities at low Q^2 . My extractions, in addition to the Bernauer and the Qattan-II extractions, are the only extractions that predict positive ratio at low Q^2 . However, the Qattan-II extractions predict rather a linear behavior. As Q^2 increases, the ratio decreases and changes sign, as seen in previous low Q^2 calculations [29,44,45,55,64,65], where it starts to increase slowly in magnitude where it becomes linear. My results are in good qualitative agreement with previous phenomenological extractions as all extractions yield similar slopes. The Arrington parametrization, on the other hand, predicts somewhat larger slope as the recoil-polarization ratio R was corrected for TPE corrections which reduces R as measured in polarization experiments. The ABGG fit shows essentially no Q^2 dependence as the Q^2 dependence of the TPE correction was taken as the dipole parametrization $G_D(Q^2) = (1 + Q^2/[0.71 (\text{GeV}/c)^2])^{-2}$ which is a nearly constant fractional correction to σ_R at large Q^2 with σ_R being dominated by $G_M^p \approx \mu_p G_D$.

Figure 2 shows the ratio $R_{e^+e^-}$ as a function of ϵ as extracted from this work for a range of Q^2 values. In addition, I compare the results to the previously mentioned phenomenological extractions and fits as well as to TPE hadronic calculations from Ref. [63] “AMT” (short-dashed red line). The curves are the same as in Fig. 1. At low Q^2 , the ratio $R_{e^+e^-}$ as extracted from this work is below unity and behaves linearly with ϵ . In general, my extractions are in good agreement with the Bernauer and the Qattan-II extractions as well as with AMT hadronic TPE calculations although the Qattan-II extractions show a strong nonlinearity at low ϵ . On the other hand, the Arrington, ABGG, and Qattan-I extractions all predict a ratio above unity with strong nonlinearity at low Q^2 and low ϵ seen in the Arrington and the ABGG extractions. Note that parametrizations where the TPE correction applied is linear or roughly linear function times $(G_M^p)^2$ will yield a strong nonlinear behavior for the ratio $R_{e^+e^-}$ at low Q^2 . It should be noted that the TPE contribution relative to $(G_M^p)^2$ is linear, but $(G_E^p)^2$ dominates σ_R at very low Q^2 , except for $\epsilon \rightarrow 0$, strongly suppressing TPE as a fractional contribution as one moves away from $\epsilon = 0$. With increasing Q^2 , the ratio increases slowly and changes sign, above unity, where it behaves linearly with ϵ in good qualitative agreement with previous extractions and TPE hadronic calculations except for the ABGG fit which shows essentially no Q^2 dependence.

In Fig. 3 I compare my predictions of the ratio $R_{e^+e^-}$ to the world data from Refs. [51,53,54,58,66–74], and to several previous phenomenological extractions and fits from Refs. [39,42,44,48,62], as well as TPE hadronic calculations from Ref. [63] at the Q^2 value listed in the figure. The measurement and the Q^2 value(s) are given in $(\text{GeV}/c)^2$. The two recent measurements from the CLAS collaboration [53] and the VEPP-3 collaboration [54] have provided significantly more precise measurements at $Q^2 \approx 1.0$ and $1.5 (\text{GeV}/c)^2$. They show a clear ϵ dependence, consistent with the form factor discrepancy at Q^2 values of 1.0 – $1.6 (\text{GeV}/c)^2$, providing

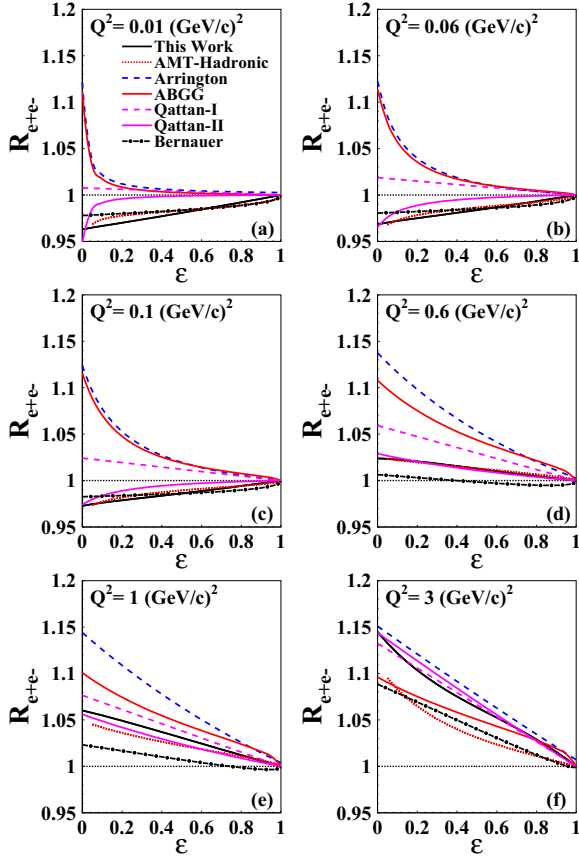


FIG. 2. The ratio $R_{e^+e^-}$ as a function of ε as extracted from this work (solid black line) for a range of Q^2 values listed in the figure. Also shown are previous TPE hadronic calculations AMT [63] (dashed red line) and phenomenological extractions and fits: ABGG [62] (solid red line), Arrington [39] (dashed blue line), Qattan-I [42] (dashed magenta line), Qattan-II [44] (solid magenta line), and Bernauer [48] (dashed-dotted black line).

evidence for nonzero TPE at larger Q^2 values and a change of sign from the exact calculations at $Q^2 = 0$ [57] which is consistent with my predictions. My results are slightly larger than the direct measurements at $1.0(\text{GeV}/c)^2$ from Ref. [54], but otherwise in very good quantitative agreement with existing data. On the other hand, the direct measurements by the OLYMPUS collaboration [58] at Q^2 values of $0.165\text{--}2.038(\text{GeV}/c)^2$ are below my predictions at larger Q^2 values, as well as TPE calculations from Refs. [59,63] and phenomenological extractions and fits from Refs. [39,42,44,62].

IV. CONCLUSIONS

In conclusion, I used a new parametrization of the TPE corrections to electron-proton elastic scattering cross section to predict the ratio of positron-proton and electron-proton scattering cross sections, $R_{e^+e^-}$. I compared the results to several previous phenomenological extractions and fits, TPE hadronic calculations, and world data on $R_{e^+e^-}$. At low Q^2 , the ratio as extracted from this work is below unity and behaves linearly with ε in agreement with phenomenological

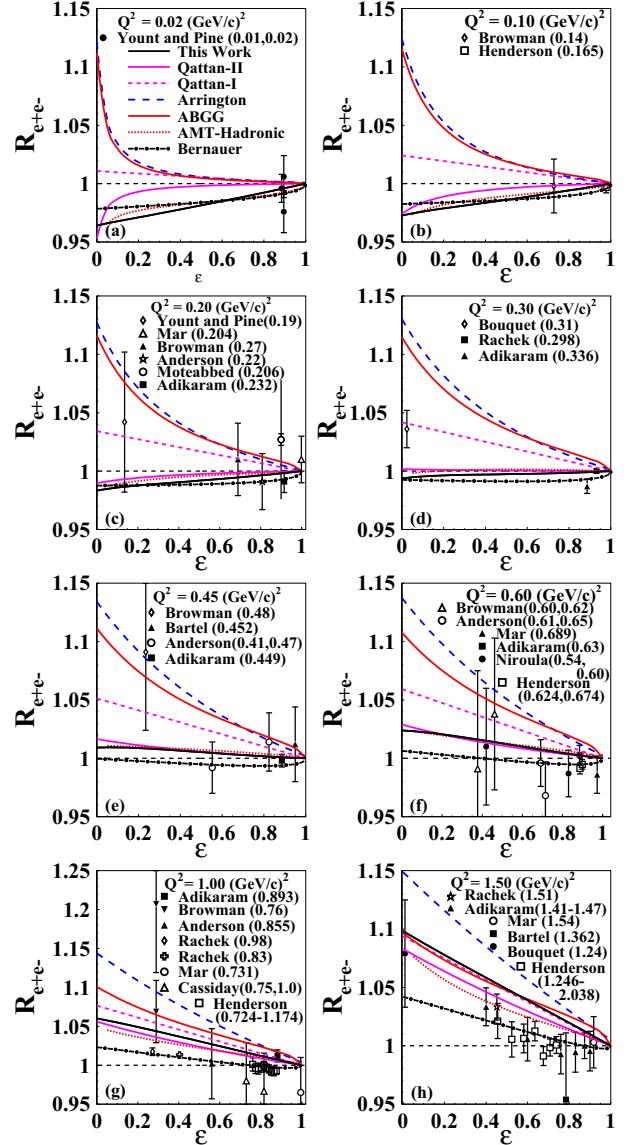


FIG. 3. The ratio $R_{e^+e^-}$ as a function of ε as extracted from this work (solid black line) at the Q^2 values listed in the figure. Also shown are previous TPE hadronic calculations AMT [63] (dashed red line) and several previous phenomenological extractions and fits: ABGG [62] (solid red line), Arrington [39] (dashed blue line), Qattan-I [42] (dashed magenta line), Qattan-II [44] (solid magenta line), and Bernauer [48] (dashed-dotted black line). The data points are direct measurements of $R_{e^+e^-}$ [51,53,54,58,66–74]. For the world data, the measurement and the Q^2 value(s) are given in $(\text{GeV}/c)^2$.

extractions from Refs. [44,48] and TPE hadronic calculations from Ref. [63]. The ratio increases slowly and changes sign, above unity, where it behaves linearly with ε at larger Q^2 values in good qualitative agreement with all previous phenomenological extractions shown from Refs. [39,42,44,48,62] and TPE hadronic calculations [63]. While my predictions are in generally good agreement with existing world data, including the recent direct measurements [53,54] which show a clear ε dependence, providing evidence for nonzero TPE at larger

Q^2 values and a change of sign from the exact calculations at $Q^2 = 0$ [57], they are larger than the new direct measurements from Ref. [58] at larger Q^2 values. Finally, as the majority of the $R_{e^+e^-}$ data are taken for $Q^2 < 2.1$ (GeV/c)² which is below where the discrepancy between the cross section and recoil-polarization measurements on the ratio $\mu_p G_E^p / G_M^p$ is significant, the assumption that TPE corrections could account

for the discrepancy remains an open question and future experiments at larger Q^2 values are clearly needed.

ACKNOWLEDGMENTS

The author acknowledges the support provided by Khalifa University of Science and Technology.

-
- [1] M. N. Rosenbluth, *Phys. Rev.* **79**, 615 (1950).
 [2] N. Dombey, *Rev. Mod. Phys.* **41**, 236 (1969).
 [3] A. I. Akhiezer and M. P. Rekalov, *Sov. J. Part. Nucl.* **4**, 277 (1974).
 [4] R. G. Arnold, C. E. Carlson, and F. Gross, *Phys. Rev. C* **23**, 363 (1981).
 [5] J. Arrington, C. Roberts, and J. Zanotti, *J. Phys. G* **34**, S23 (2007).
 [6] C. Perdrisat, V. Punjabi, and M. Vanderhaeghen, *Prog. Part. Nucl. Phys.* **59**, 694 (2007).
 [7] M. E. Christy *et al.*, *Phys. Rev. C* **70**, 015206 (2004).
 [8] I. A. Qattan *et al.*, *Phys. Rev. Lett.* **94**, 142301 (2005).
 [9] O. Gayou *et al.*, *Phys. Rev. Lett.* **88**, 092301 (2002).
 [10] O. Gayou *et al.*, *Phys. Rev. C* **64**, 038202 (2001).
 [11] A. J. R. Puckett *et al.*, *Phys. Rev. C* **85**, 045203 (2012).
 [12] V. Punjabi *et al.*, *Phys. Rev. C* **71**, 055202 (2005); **71**, 069902(E) (2005).
 [13] S. Strauch *et al.*, *Phys. Rev. Lett.* **91**, 052301 (2003).
 [14] A. J. R. Puckett *et al.*, *Phys. Rev. Lett.* **104**, 242301 (2010).
 [15] G. Ron *et al.*, *Phys. Rev. C* **84**, 055204 (2011).
 [16] M. K. Jones *et al.*, *Phys. Rev. C* **74**, 035201 (2006).
 [17] G. MacLachlan *et al.*, *Nucl. Phys. A* **764**, 261 (2006).
 [18] M. Paolone *et al.*, *Phys. Rev. Lett.* **105**, 072001 (2010).
 [19] X. Zhan *et al.*, *Phys. Lett. B* **705**, 59 (2011).
 [20] C. B. Crawford *et al.*, *Phys. Rev. Lett.* **98**, 052301 (2007).
 [21] T. Pospisil *et al.*, *Eur. Phys. J. A* **12**, 125 (2001).
 [22] B. D. Milbrath *et al.* (Bates FPP Collaboration), *Phys. Rev. Lett.* **80**, 452 (1998); **82**, 2221 (1999).
 [23] C. E. Carlson and M. Vanderhaeghen, *Annu. Rev. Nucl. Part. Sci.* **57**, 171 (2007).
 [24] J. Arrington, P. Blunden, and W. Melnitchouk, *Prog. Part. Nucl. Phys.* **66**, 782 (2011).
 [25] P. A. M. Guichon and M. Vanderhaeghen, *Phys. Rev. Lett.* **91**, 142303 (2003).
 [26] J. Arrington, *Phys. Rev. C* **68**, 034325 (2003).
 [27] J. Arrington, *Phys. Rev. C* **69**, 022201(R) (2004).
 [28] P. G. Blunden, W. Melnitchouk, and J. A. Tjon, *Phys. Rev. Lett.* **91**, 142304 (2003).
 [29] P. G. Blunden, W. Melnitchouk, and J. A. Tjon, *Phys. Rev. C* **72**, 034612 (2005).
 [30] S. Kondratyuk, P. G. Blunden, W. Melnitchouk, and J. A. Tjon, *Phys. Rev. Lett.* **95**, 172503 (2005).
 [31] Y. C. Chen, A. Afanasev, S. J. Brodsky, C. E. Carlson, and M. Vanderhaeghen, *Phys. Rev. Lett.* **93**, 122301 (2004).
 [32] D. Borisyuk and A. Kobushkin, *Phys. Rev. C* **74**, 065203 (2006).
 [33] D. Borisyuk and A. Kobushkin, *Phys. Rev. C* **78**, 025208 (2008).
 [34] E. Tomasi-Gustafsson and G. I. Gakh, *Phys. Rev. C* **72**, 015209 (2005).
 [35] I. A. Qattan, Ph.D. thesis, Northwestern University (2005), [arXiv:nucl-ex/0610006](https://arxiv.org/abs/nucl-ex/0610006).
 [36] V. Tsvakis *et al.*, *Phys. Rev. C* **73**, 025206 (2006).
 [37] Y.-C. Chen, C.-W. Kao, and S.-N. Yang, *Phys. Lett. B* **652**, 269 (2007).
 [38] D. Borisyuk and A. Kobushkin, *Phys. Rev. C* **76**, 022201(R) (2007).
 [39] J. Arrington, *Phys. Rev. C* **71**, 015202 (2005).
 [40] J. Guttmann, N. Kivel, M. Meziane, and M. Vanderhaeghen, *Eur. Phys. J. A* **47**, 77 (2011).
 [41] I. A. Qattan and A. Alsaad, *Phys. Rev. C* **83**, 054307 (2011); **84**, 029905(E) (2011).
 [42] I. A. Qattan, A. Alsaad, and J. Arrington, *Phys. Rev. C* **84**, 054317 (2011).
 [43] I. A. Qattan and J. Arrington, *Phys. Rev. C* **86**, 065210 (2012).
 [44] I. A. Qattan, J. Arrington, and A. Alsaad, *Phys. Rev. C* **91**, 065203 (2015).
 [45] D. Borisyuk and A. Kobushkin, *Phys. Rev. C* **75**, 038202 (2007).
 [46] M. Meziane *et al.*, *Phys. Rev. Lett.* **106**, 132501 (2011).
 [47] M. P. Rekalov and E. Tomasi-Gustafsson, *Eur. Phys. J. A* **22**, 331 (2004).
 [48] J. C. Bernauer *et al.* (A1 Collaboration), *Phys. Rev. C* **90**, 015206 (2014).
 [49] D. Borisyuk and A. Kobushkin, *Phys. Rev. D* **83**, 057501 (2011).
 [50] I. A. Qattan, *Phys. Rev. C* **95**, 055205 (2017).
 [51] J. Mar *et al.*, *Phys. Rev. Lett.* **21**, 482 (1968).
 [52] J. Arrington, *Phys. Rev. C* **69**, 032201(R) (2004).
 [53] D. Adikaram *et al.* (CLAS Collaboration), *Phys. Rev. Lett.* **114**, 062003 (2015).
 [54] I. A. Rachev *et al.* (VEPP-3 Collaboration), *Phys. Rev. Lett.* **114**, 062005 (2015).
 [55] J. Arrington and I. Sick, *Phys. Rev. C* **70**, 028203 (2004).
 [56] H.-Q. Zhou and S. N. Yang, *Eur. Phys. J. A* **51**, 105 (2015).
 [57] W. A. McKinley and H. Feshbach, *Phys. Rev.* **74**, 1759 (1948).
 [58] B. S. Hendrson *et al.* (OLYMPUS Collaboration), *Phys. Rev. Lett.* **118**, 092501 (2017).
 [59] P. Blunden (private communication) (2016).
 [60] O. Tomalak and M. Vanderhaeghen, *Eur. Phys. J. A* **51**, 24 (2015).
 [61] A. Afanasev, P. G. Blunden, D. Hasell, and B. A. Raue, *Prog. Part. Nucl. Phys.* **95**, 245 (2017).
 [62] W. M. Alberico, S. M. Bilenyk, C. Giunti, and K. M. Graczyk, *Phys. Rev. C* **79**, 065204 (2009).
 [63] J. Arrington, W. Melnitchouk, and J. A. Tjon, *Phys. Rev. C* **76**, 035205 (2007).
 [64] J. Arrington, *J. Phys. G* **40**, 115003 (2013).
 [65] N. Kivel and M. Vanderhaeghen, *Phys. Rev. Lett.* **103**, 092004 (2009).
 [66] D. Yount and J. Pine, *Phys. Rev.* **128**, 1842 (1962).

- [67] A. Browman, F. Liu, and C. Schaerf, *Phys. Rev.* **139**, B1079 (1965).
- [68] R. L. Anderson *et al.*, *Phys. Rev. Lett.* **17**, 407 (1966).
- [69] R. L. Anderson *et al.*, *Phys. Rev.* **166**, 1336 (1968).
- [70] W. Bartel *et al.*, *Phys. Lett. B* **25**, 242 (1967).
- [71] B. Bouquet *et al.*, *Phys. Lett. B* **26**, 178 (1968).
- [72] M. Moteabbed *et al.*, *Phys. Rev. C* **88**, 025210 (2013).
- [73] M. Niroula, Ph.D. thesis, Old Dominion University (2010), INSPIRE-1288437.
- [74] G. Cassiday *et al.*, *Phys. Rev. Lett.* **19**, 1191 (1967).